



**CLARIS | LPB**

**CLARIS | LPB**

A Europe-South America Network for Climate Change Assessment

And Impact studies in La Plata Basin

<http://www.claris-eu.org>

**Deliverables**



Instrument: **SP1 Cooperation**

Thematic Priority: **Priority Area 1.1.6.3 "Global Change and Ecosystems"**

**FP7 Collaborative Project – Grant Agreement 212492**

**CLARIS LPB**

**A Europe-South America Network for Climate Change Assessment and Impact Studies in La Plata Basin**

**DELIVERABLES**

**D6.3: Report on the relationships between the occurrence of extreme events over LPB and the large scale circulation and SSTs anomalies in both observations and model simulations and on the role of land-atmosphere feedbacks on the LPB extremes occurrence.**

Due date of deliverable: Month 36

Start date of project: **01/10/2008**

Duration: **4 years**

Organization name of lead contractor for this deliverable: CONICET

Deliverable No	Deliverable title	WP	Lead beneficiary	Estimated indicative person-months (permanent staff)	Nature	Dissemination level	Delivery date
D6.3	Report on the relationships between the occurrence of extreme events over LPB and the large scale circulation and SSTs anomalies in both observations and model simulations and on the role of land-atmosphere feedbacks on the LPB extremes occurrence.	WP 6	P13-CONICET P9-INPE	23,20	R	PU	36

## 1. Introduction

The main objective of WP6 is to elucidate the climate processes that are associated with extreme hydro-climate conditions over LPB region, considering both the role of the large scale forcing and the local interactions, and the way in which the frequency and intensity of such cases may change according to different projections of global climate change. Activities related with this deliverable are mainly related with task 6.1.

## 2. Report on atmospheric features, land surface-atmosphere, and ocean-atmosphere feedbacks, associated with the occurrence of extremes in precipitation and temperature.

Partners involved in this deliverable are the CMCC, UBA, CONICET, UFP and INPE. A resume of the main results group by group are summarized as follows.

**CONICET, UBA and CMCC (Andrea Carril, Annalisa Cherchi, Claudio Menéndez, Pablo Zaninelli and Laura Zamboni)**

### Links between tropical Pacific SSTs anomalies and temperature extremes over South America

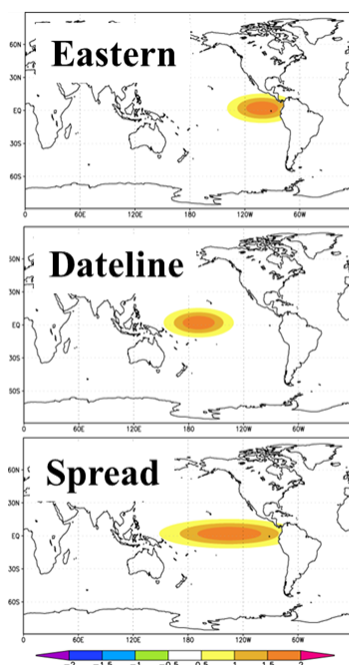


Figure 1: Idealized forcing

The influence of the phase and location of tropical SSTs anomalies on the frequency of occurrence of extreme temperatures over South America is investigated. The motivation of this work is the shift in behavior, frequency and characteristics of El Niño events over recent years (e.g. Ashok and Yamagata 2009, Yeh et al. 2009).

The study is conducted on the basis of seven idealized experiments, by integrating ECHAM4 AGCM at T106 resolution. The control run is a 30-year length experiment forced with climatological SST without interannual variability (i.e., it simulates atmospheric internal variability). The six sensitivity experiments are 30-year length each one, being forced with climatological SST everywhere, except in the tropical Pacific where idealized warm/cold anomalies are superimposed in the eastern basin (WE/CE), in the dateline region (WD/CD) and spread across both regions (SW/SC). These forcing were turned on during October-November, when the Southern Hemisphere mean flow lets an optimum and fast propagation of meridional waves far from the source.

The analysis of the experiments focuses on the occurrence of temperature extremes over South America. The control run is used to estimate the percentiles of reference, while extremes are measured as number of days exceeding the thresholds of the control run. Daily values of maximum and minimum surface temperature (TX, TN) were analyzed. Results of

Deliverables

occurrence of extremes in different idealized configurations are expressed as exceeding frequencies, in percentage terms.

Preliminary results suggest that temperature extremes over South America are sensitive to the phase and location of the tropical forcing. In some continental regions, the statistical distribution of TX moves towards higher temperatures when a tropical warm pool is turned on (e.g., northern of about 30°S in SW case, northern of about 35°S in DW and both, northern of about 20°S and southern of about 40°S in EW experiment, see figure 2). Although the opposite phase in the forcing produces roughly symmetrical patterns in the frequency of occurrence of extremes, the sensitivity is greater for positive than for negative pools. On the other hand, sensitivity of extremes in TN is similar to that observed in TX, but the signal maximizes (and it is enhanced) in tropical regions, while in La Plata Basin and in Patagonia the signal vanishes. The related changes in the occurrence of extremes could be partially explained trough anomalies in the tropical-extratropical teleconnections and in other large-scale patterns. On other words, we suggest that the increasing frequency of Central Pacific El Nino (CP)-like events (Yeh et al. 2009) could particularly impact in the frequency of occurrence of extreme temperature events along the entire South American region. Results could be further projected in the context of potential global warming associated with increasing frequency of CP-like events or in the context of decadal variations in the character of ENSO events.

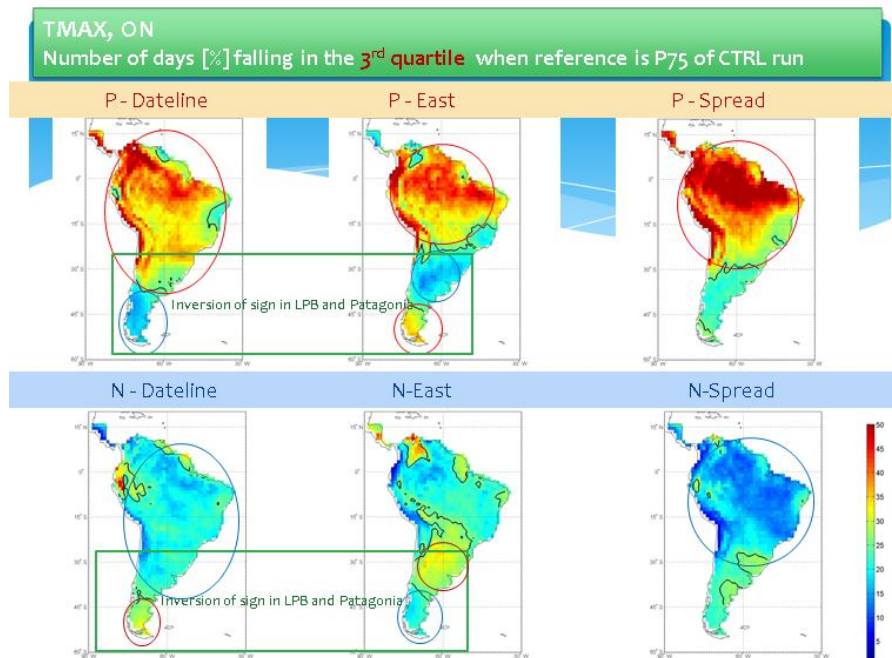


Figure 2: Sensitivity of maximum temperature to the tropical SST anomaly. Sensitivity is expressed as frequency of days falling in the 3<sup>rd</sup> quartile. Threshold of reference is the percentile 75 of the control run.

**UFP (Alice M. Grimm, Renata G. Tedeschi, Rafaela A. Flach, Lais Drozd )**

**Influence of canonical ENSO events on the frequency and intensity of extreme precipitation events in South America**

Grimm and Tedeschi (2009) carried out the assessment of ENSO influence on the frequency and intensity of extreme precipitation events in South America, for each month of the ENSO cycle, based on a large set of daily station rainfall data, and compared with the influence of ENSO on the monthly total rainfall. Significant ENSO signals in the frequency of extreme events are found over extensive regions of South America during different periods of the ENSO cycle. Although ENSO related changes in intensity show less significance and spatial coherence, they are robust in several regions, especially in the La Plata Basin.

The ENSO-related changes in the frequency of extreme rainfall events are generally coherent with changes in total monthly rainfall. However, significant changes in extremes are much more extensive than the corresponding changes in monthly rainfall, because the highest sensitivity to ENSO resides in the extreme range of daily precipitation in several regions of South America, especially the La Plata Basin. A preliminary analysis of the atmospheric anomalies associated with extreme precipitation events in the regions most affected during ENSO episodes was carried out. The stronger impact of ENSO on the extreme tail of the daily precipitation than on monthly rainfall totals in several regions of South America, especially the La Plata Basin, is related to the effect that ENSO has on the circulation anomalies associated with the extreme events in these regions, enhancing or hampering the main mechanisms leading to extreme events in these regions.

**UFP and INPE/CPTEC (Alice M. Grimm, Renata G. Tedeschi and Iracema Cavalcanti)**

**Influence of different types of ENSO (Central and East Pacific) on the seasonal precipitation and frequency of extreme precipitation events in South America and verification of this influence in climate models.**

Different types of ENSO events, with stronger SST anomalies in the central or in the eastern Pacific, are able to produce different impacts on rainfall over the La Plata Basin (Tedeschi, Cavalcanti and Grimm, 2011). There are also significant differences regarding the impact on the frequency of extreme events, especially in the La Plata Basin, in which very catastrophic floods have happened during austral autumns of El Niño events. The discrimination of these events according to their maximum SST in the region Niño 3.4 or in the region Niño 3 shows that this impact is greater in the middle La Plata Basin in the eastern Pacific category (Figure 3). The associated teleconnections explain this difference.

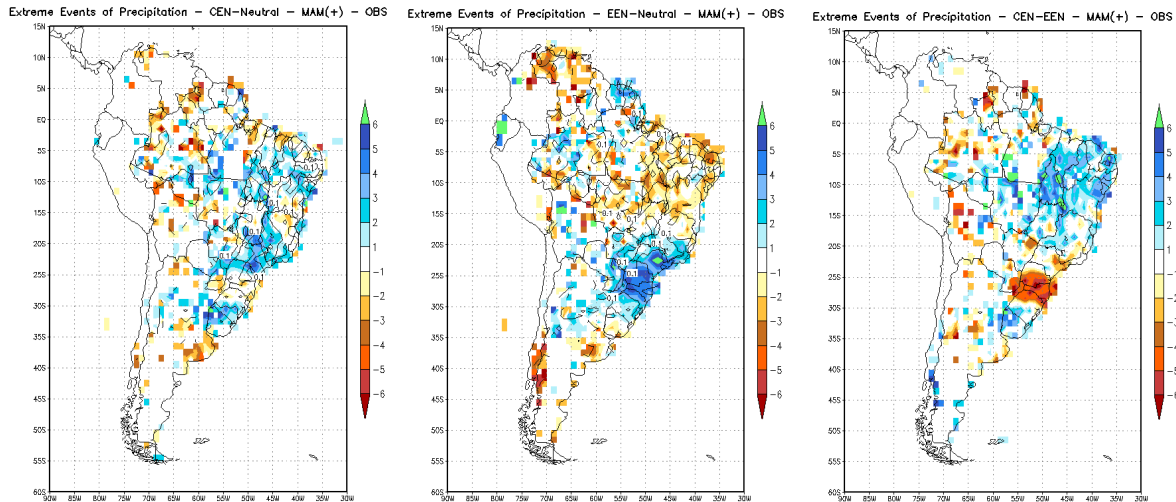


Fig. 3. (Left panel) Differences between average numbers of extreme rainfall events during austral autumns following the onset of central Pacific El Niño events and during neutral years; (central panel) the same, but for eastern Pacific El Niño events and neutral years; (right panel) the same but for central Pacific El Niño and eastern Pacific El Niño. (From Tedeschi, Grimm and Cavalcanti 2011)

### UFP (Alice M. Grimm, Renata G. Tedeschi, Rafaela A. Flach, Lais Drozd )

#### Preliminary assessment of the influence of interdecadal oscillations on the frequency of extreme events.

Interdecadal variability of precipitation is also very significant in the La Plata Basin (Grimm and Saboia, 2011). During its opposite phases (principal components beyond  $\pm 0.7$  standard deviation) significant impact is, as for ENSO, generally more extensive on the frequency of extreme events than on the seasonal (or monthly) total precipitation, and both variations are generally coherent. The distributions of daily rainfall during opposite phases show that in most of the regions the frequencies of heavy rainfall undergo greater relative changes than the frequencies of light or moderate rain, and in many cases they change in opposite sense. Fig. 4, from Grimm and Drozd (2011), shows that in the positive (negative) phase of the first interdecadal variability mode of spring precipitation the frequencies of light precipitation in the southernmost part of Brazil increase (decrease) a little but the frequencies of heavy precipitation decrease (increase) much more. Since changes in total precipitation and in the frequency of extreme events are generally coherent (although not always both significant), this indicates that the changes in total rainfall are mainly due to changes in heavy precipitation. This is an important aspect, since the most dramatic consequences of climate variability result from changes in extreme events.

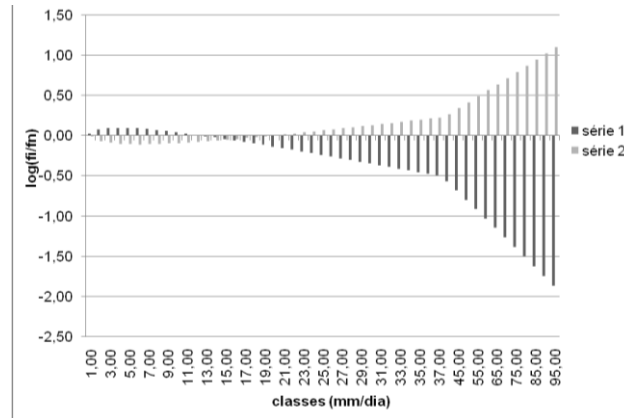


Fig. 4. Relative changes in the PDF of observed daily rainfall in a grid box  $1^{\circ} \times 1^{\circ}$  in southern Brazil, due to the first interdecadal variability mode of spring precipitation. The black (white) bars represent the logarithm of the ratio between frequencies of daily rainfall during the positive (negative) phase of this mode and during neutral years. The frequencies are given by gamma distributions fitted to the observed daily precipitation during each category of year (positive phase, negative phase and neutral years). (From Grimm and Drozd 2011)

### INPE/CPTEC and UFPR (Renata Tedeschi, Iracema FA Cavalcanti, Alice Grimm) The influence of ENOS modified Modoki and Canonical on La Plata basin precipitation

Sea Surface Temperature (SST) anomalies in the Pacific Ocean in ENSO episodes display different positions in some years. The objective of this study was to compare results from Canonical and a Modified Modoki ENSO in the four seasons and analyze their influences on La Plata basin precipitation over South America (SA). The criterion to define a Canonical El Niño (EN) (La Niña - LN) is based on seasonal SST anomalies in the area  $90^{\circ}\text{W}-140^{\circ}\text{W}$  and  $5^{\circ}\text{N}-5^{\circ}\text{S}$ , which is part of Niño 3 region. EN (LN) years are selected when the seasonal SST anomaly in this area is above (below)  $0,7\sigma$  (where  $\sigma$  is the standard deviation for the season). A modified Modoki EN (LN) is selected when the Modoki index is above (below)  $0,7\sigma$  of this index series and the SST anomaly in the area A ( $165^{\circ}\text{E}-140^{\circ}\text{W}$ ,  $10^{\circ}\text{S}-10^{\circ}\text{N}$ ) is greater (lesser) than  $0,7\sigma$  of the anomaly SST series. During the Canonical EN (LN) there is precipitation increase (decrease) on the La Plata Basin (LPB) and a decrease (increase) on northern South America, in all seasons. In MModoki ENSO, these typical patterns are not observed. Differences or similarities of precipitation anomalies over South America between Canonical and MModoki cases occur in different areas and different seasons. The differences in tropical South America precipitation during the two ENSO types are related to the differences in the Walker circulation during each ENSO type. In extratropical South America, the precipitation differences are due to differences in the Pacific wavetrains and differences in the moist flux intensity over the continent. These results were included in a submitted manuscript Tedeschi et al., 2011.

## INPE/CPTEC (Iracema FA Cavalcanti)

### Extreme precipitation over two sectors of La Plata Basin and associated large scale features

Large scale patterns in extreme cases over the northern and southern sectors were analyzed comparing observations and CPTEC AGCM results. Composites of extreme and severe wet cases and composites of extreme and severe dry cases in the northern LPB sector and in the southern sector showed the dipole behavior between the two sectors. The CPTEC AGCM and HADCM3 reproduce this behavior (Figure 5). The global precipitation analyses show that in these cases there is also a north-south dipole over the western South Pacific, which inverts following the dipole inversion over South America. Wet precipitation composites show the existence of wavetrains from the western tropical Pacific to South America (PSA-type) in the case of extreme and severe wet cases in the northern sector. For the southern sector, the wavetrain occurs from the Indian Ocean to South America. Some of these large scale characteristics are reproduced by the models but the wavetrains are not organized as in the observations.

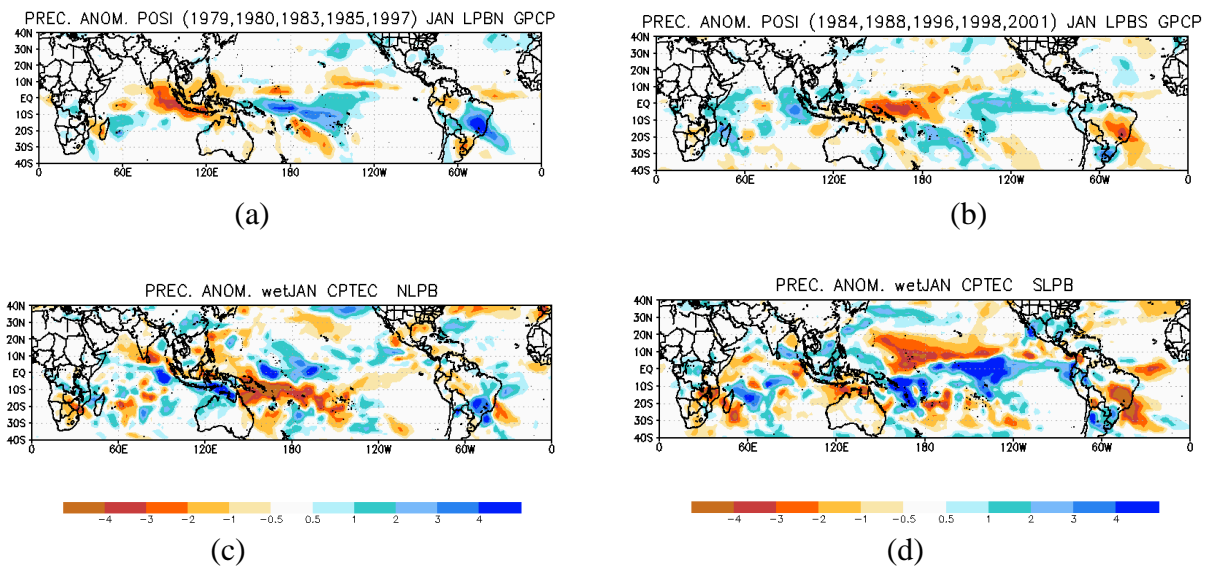


Figure 5- Precipitation anomalies composites of wet extreme and severe cases of precipitation, in January, over the northern (a, c) and southern (b,d) La Plata Basin sectors. GPCP (a,b), CPTEC AGCM (c,d).

## UBA (Federico Robledo and Olga Penalba)

### Global and regional features and impacts on extreme rainfall over Argentina.

Planetary and regional features of the atmospheric circulation that impact in the extreme rainfall on Argentina were analyzed. The analysis has been made on the basis of the leading pattern of covariability between spring the daily intensity of extreme rainfall (DIER) in Argentina and sea surface temperature (SST) for all the oceans from 17.5° N to 90° S. This analysis was performed using a Singular Values Decomposition (SVD) for spring in the period 1962 to 2005. Two data sets were used to the SVD analysis: monthly SST from the Kaplan SST V2 from the NCEP/NCAR and high quality daily rainfall for 35 surface stations from the National Weather Service of Argentina distributed throughout the country. The monthly mean of daily intensity of extreme rainfall index (DIER) is the quotient between the monthly accumulated extreme rainfall (AE) and the number of days with extreme precipitation events per month (PE). We consider extreme daily precipitation when rainfall is greater than the mean 75th daily percentile for the period 1961 to 2000. Regression maps between SVD times series and relevant

Deliverables

variables like meridional wind at 200 hPa and 850 hPa, and geopotential height to 500 hPa were performed in order to describe leading patterns signal on the southern hemisphere circulation (Figure 6). The three leading SVD modes of the coupled SST and DIER variations account around 72 percent for spring of the total square covariance (TSC). The first mode of spring explains 45% of TSC. Spatial pattern of the leading mode are associated with SST anomalies resembling those typically linked to ENSO with 4-year temporal cycles and enhanced DIER in central and eastern Argentina. Regression maps of circulation anomalies depict Rossby-like wave trains emanating from central tropical Pacific and equatorial Indian oceans, in a similar way than those previously identified by other papers as promoted by ENSO events.

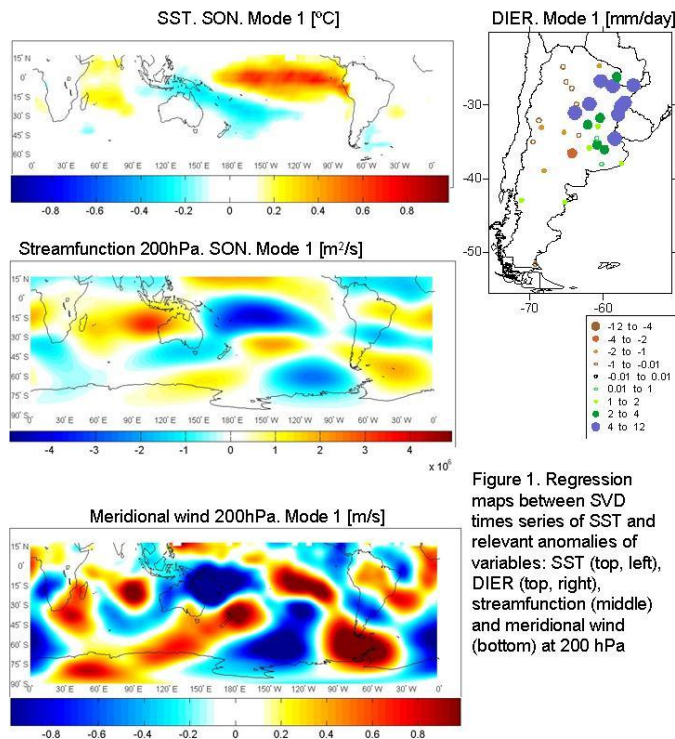


Figure 1. Regression maps between SVD times series of SST and relevant anomalies of variables: SST (top, left), DIER (top, right), streamfunction (middle) and meridional wind (bottom) at 200 hPa

Fig.6.. Regression maps between SCD time series of SST (top, left), DIER (top, right), streamfunction at 200 hPa (middle), and meridional wind at 200 hPa (bottom).

The second SVD mode that explains 17% of TSC, presents an anomalous cooling in the tropical Atlantic Ocean as well as in the Indonesian Sea associated with low DIER over northeastern Argentina. This mode shows a significant decadal variability with two sub-periods: 8 years and 12 years. An upper-level cyclonic circulation anomaly is observed southward of the negative SST anomaly center located over the equatorial Atlantic. On the other hand, an anticyclonic circulation is identified over southeastern South America. Both features seem to be part of a Rossby-like wave train extending from western tropical Pacific Ocean arching toward South America. Evidences of an annular circulation structure are also observed over the Polar Regions in association with this particular SVD mode. The third SVD mode explains 10% of TSC and shows significant variability on periods around 14 years. A horseshoe-like shape characterizes the SST anomalies over the western Pacific related with this SVD mode while negative (positive) DIER extends over northern (central-east) Argentina. Circulation anomalies extend between New Zealand region and South America in relation to the third SVD mode.



## **CONICET and UBA (Anna Sörensson and Claudio Menéndez)** **Exploring relationships between extremes and land surface conditions**

Sörensson and Menéndez (2011) found out that heavy rainfall in Southern LPB may be partly related to land-atmosphere coupling. They calculate the coupling strength between soil moisture, evapotranspiration and precipitation for summer by analyzing ensembles of simulations performed with a RCM. The regional spatial patterns of extreme precipitation (defined as the fraction of the total seasonal precipitation that is due to the 95th percentile of daily precipitation) are well correlated with the regions of strong coupling between soil moisture and evapotranspiration over large areas of South Eastern South America. In addition, results suggest that extreme precipitation seems enhanced over regions of high soil moisture-precipitation coupling if the model includes a complete land surface-atmosphere interaction (in comparison with simulations in which the link between precipitation and soil moisture is cut through using prescribed soil moisture).

## **CONICET and UBA (Natalia Pessacg and Silvina Solman)** **Impacts of land use changes in southern South America climate for extreme climatic periods.**

This study examines the effects of land use/land cover changes (LULCC) over the climate in two important agricultural regions over southern South America, La Plata Basin and the Argentinean Pampas. In the last decade these regions have been suffered a replacement of the natural cover, mainly by the expansion of the agricultural activity, associated with an increase in the soy production. In this context and with the objective of analyze the impacts of LULCC in the southern South America climate, a series of sensitivity experiment were performed with the MM5 regional model, in which the natural cover was replaced by crop (CROP experiments) during different years related with extreme phases of the El Niño-Southern Oscillation (ENSO).

The experiments were analyzed for the austral summer during three particular periods 1996-1997, 1997-1998 and 1999-2000, a non-ENSO year and extremes El Niño (EN) and La Niña (LN) years, respectively.

Experiments showed a decrease of temperature, smaller than 1°C, when crop replaces the natural cover during the summer of the neutral and EN years over the north of Argentina and Paraguay (Fig.7). Though this value is close to the internal variability the signal is consistent for every pair of the ensemble members. For LN year the impacts of LULCC is quite different with regions of warming and cooling over the north and central Argentina, Paraguay and part of Bolivia.

Over the region where the main changes in 2meter temperature were localized (Fig7), there is a shift from savanna and cropland/woodland mosaic to dry land crop. This shift leads to a decrease of albedo and an increase of emissivity, both driving to a decrease in the total radiation energy budget at surface, which, in turn, leads to an increase of the latent heat flux and a decrease of the sensible heat flux, consequently, decreasing the Bowen ratio. Both mechanisms can explain the cooling in the CROP scenario with respect to the control scenario during the neutral and EN years. On one hand the increase in latent heat flux leads to an increase in the evaporative cooling and, on the other hand, the change in the energy partition that drives to a decrease of the Bowen ratio, indicate that more energy is used in transpiration and evaporation than in heating the atmosphere near to the surface. These mechanisms give a physical context to the change in temperature due to LULCC, being the magnitude of these changes smaller than the internal variability of the system, though statistically consistent.

Besides that, simulations allow us to determine the effect over the regional climate of the local and remote forcing together, and show that the interannual variability is important when assessing the strength of the impact. The cooling due to LULCC signal during El Niño year over north Argentina and Paraguay tends to weaken the strength of the interannual variability during the austral spring, which is characterized by a warm anomaly over this area. During summer, El Niño signal over the north of Argentina and Paraguay play in the same way as the LULCC signal, cooling the atmosphere near to the surface. Over the central and east of Argentina and Uruguay the interannual variability during summer presents a cold anomaly and the LULCC signal tend to enhance this effect and during La Niña there is a warming that is enhanced by the LULCC signal.

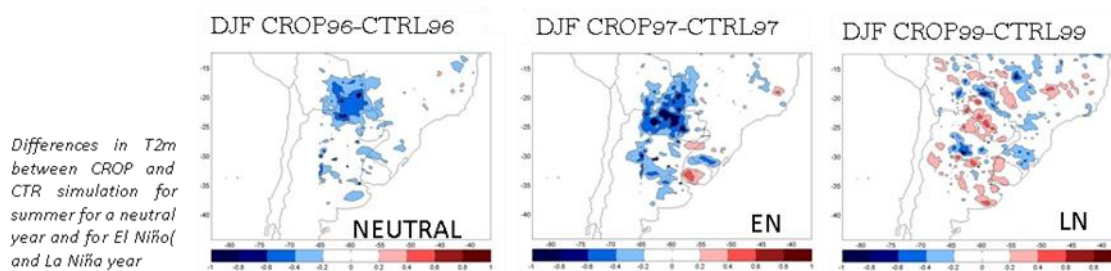


Fig. 7. Differences in T2m between CROP and CTR simulation for summer for a neutral year and for El Niño and La Niña year.

## UBA (Vanesa C. Pántano and Olga C. Penalba)

### Who is responsible for the extreme hydric condition? - Preliminary results for SUMMER

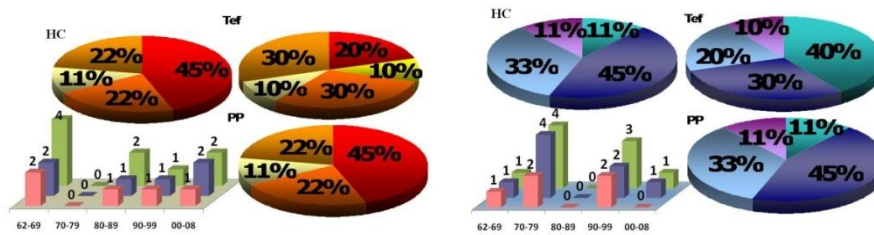
In Argentina, the region of the Cuenca del Plata is characterized by a great agriculture production without irrigation. The yields of the crops strongly depend on the variability and the interaction between the soil and the atmosphere. In particular, the temperature and the rainfall are the principal variables that influence the hydric condition of the soil. After the 50's the annual rainfall increased, displacing the agriculture border in Argentina westward, improving the agricultural production of the region. Besides, changes in the temperature were also observed during the last decades.

In this context, the extreme events play an important role in the development of the crops, producing a socio-economic impact in the affected zones.

The objective of this work is to analyze the percentages of extreme hydrological conditions in La Plata Basin over Argentina and evaluate which variable (temperature or precipitation) is responsible for those extreme conditions. The different components of the water balance are computed through the daily precipitation and effective temperature, estimated from maximum and minimum temperatures. This information, in the period 1960-2008, was provided by the National Meteorological Service and the National Institute of Agriculture Technology. Then, the soil moisture condition was computed through the hydric conditions defined as excess minus deficit.

Paso de los Libres

Deliverables



Marcos Juarez

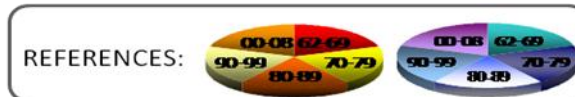
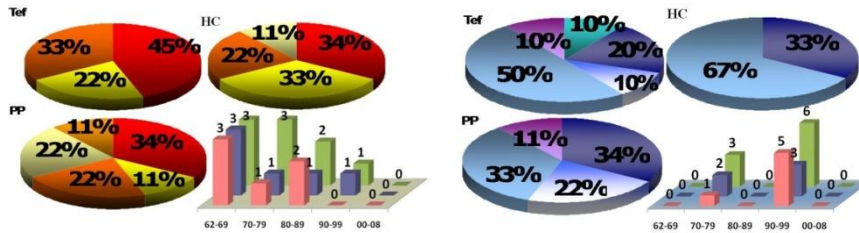


Fig. 8. Percentage of extreme unfavorable (left) and favorable (right) hydric conditions per decade (see Reference pies) and for each variable represented through pies. The Bar chart corresponds to the number of years per decade under extreme hydric conditions (HC: green bar) and which of them presented extreme precipitation (PP: blue bar) and extreme effective temperature (Tef: pink bar).

The extreme hydric conditions were defined as the values above and below the 80 and 20 percentile respectively, and the extreme unfavorable and favorable conditions were evaluated. The decadal variability of the percentage of these extreme events were also performed for the hydric conditions and compared with the results for temperature and precipitation. In order to analyze the relationship between them, the number of years per decade under extreme hydric conditions was calculated and which of them presented extreme precipitation and extreme temperature.

The results for Paso de los Libres and Marcos Juarez are shown, as an example, in figure 8. For the first station, the 60s present the major percentage of extreme unfavorable hydric condition while the 70s and 90s present the major percentage of extreme favorable hydric condition. Although the values of extreme precipitation and extreme hydric conditions are the same for each decade, they don't necessarily occur in the same year. On the other hand, for Marcos Juarez, the 60s and 70s present the major percentage of extreme unfavorable hydric conditions. While the 90s (with 67%) and 70s (with 33%) are the only decades that present extreme favorable hydric conditions. However, some cases of extreme effective temperature and extreme precipitations were observed on the other decades.

In general, a great number of favorable and unfavorable extreme events are consistent with the extreme precipitation cases in the region. Extreme Temperature seems to have a stronger influence over extreme unfavorable hydric conditions than over the extreme favorable hydric conditions. For some stations, as Marcos Juarez, a percentage of extreme precipitation and extreme temperature were observed for a particular decade while there were zero events of extreme hydric condition.

Finally, a progressive decrease of extreme unfavorable conditions and increase of extreme favorable conditions are also observed for the rest of the stations through the decades.

## MPI-M (Armelle Reca Remedio, Susanne Pfeifer and Daniela Jacob) On the relationship of low level jets and mesoscale convective systems in South America

Previous studies have indicated the importance of the strong low level winds especially during the austral summer (e.g. Marengo 2004, Vera 2006, and Salio 2007). The low level jet contributes significantly in the transport of moisture from the Amazon Basin to the La Plata Basin during summer. As the heat and moisture is advected towards the south, it initiates convection that develop into mesoscale convective systems which later on produces heavy precipitation ranging from several hours to few days. These systems cause extreme weather conditions such as flooding and thunderstorms around the La Plata Basin.

Within the framework of the project, the characteristics of the low level jets and mesoscale convective systems are analyzed using REMO2009, the latest hydrostatic version of the regional model. The domain covers the whole South American continent at  $0.44^\circ \times 0.44^\circ$  resolution with the initial and boundary conditions driven by the ERA-Interim reanalysis with resolution of about  $0.7^\circ$ . The period covered in this study is from 1989 to 2008. Model-derived winds are compared with reanalysis and observations from the ERA-INTERIM and SALLJEX. Model-derived precipitation and outgoing long wave radiation are compared with satellite estimates of NCEP, TRMM and MERGE, which is a hybrid rainfall data from rainge gauge observations merged with TRMM.

**Low. Level jets.** The methods that were used in detecting low level jets are the criteria based on Bonner and two modified Bonner criteria. The different criterion utilizes the characteristics of winds at 850 hPa and wind shear between 850 hPa and 700 hPa as listed in Table 1. In addition to the list, only the meridional winds that are greater than the zonal winds are selected. These three criteria are used in calculating the occurrences of the low level jet at grid points closest to radiosonde observations.

*Table 1. Different low level jet criteria*

Criteria	References	Winds at 850 hPa	Wind shear between 850 hPa and 700 hPa
BC: Bonner	Bonner 1968	Northerly wind speeds $\geq 12$ m/s	Shear $\geq 6$ m/s
MB1: Modified Bonner 1	Sugahara et al, 1994	Northerly meridional wind velocity $\leq -8$ m/s	Shear $\geq 2$ m/s
MB2: Modified Bonner 2	Rozante and Cavalcanti, 2008	Northerly meridional wind velocity $\leq -12$ m/s	Shear $\geq 6$ m/s

We have calculated the annual cycle of the low level jet occurrences over 8 stations listed by Marengo et al, 2004. The winds in the reanalysis indicate that the MB1 has more low level jet episodes compared to BC and MB2. From Table 1, it can be inferred that MB1 has less strict criterion in selecting low level jets compared to the other two. Evaluating the low level jet events in a grid point close to the radiosonde station in Santa Cruz, Bolivia, REMO and ERA-Interim have a similar total number of monthly events. Considering just the BC criterion and comparing it to a previous study (Marengo et al, 2004), the number of events detected in the reanalysis and REMO have a larger number of events during the austral winter time (Figure 9). This could be attributed to the fact that Marengo et al (2004) is using the NCEP-NCAR Reanalysis which has a coarser resolution at  $2.5^\circ$  and at a different time period (1950-2000). In NCEP-NCAR, the grid point located near the station is about 80 km while the reanalysis and the model has a distance of about less than 10km.

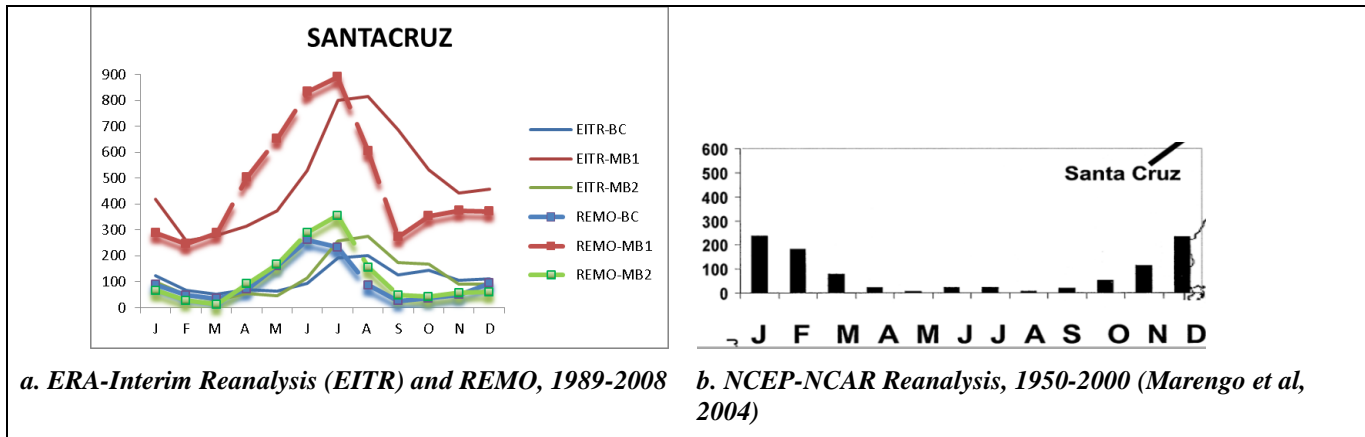


Figure 9. Total monthly low level jet events for Santa Cruz, Bolivia.

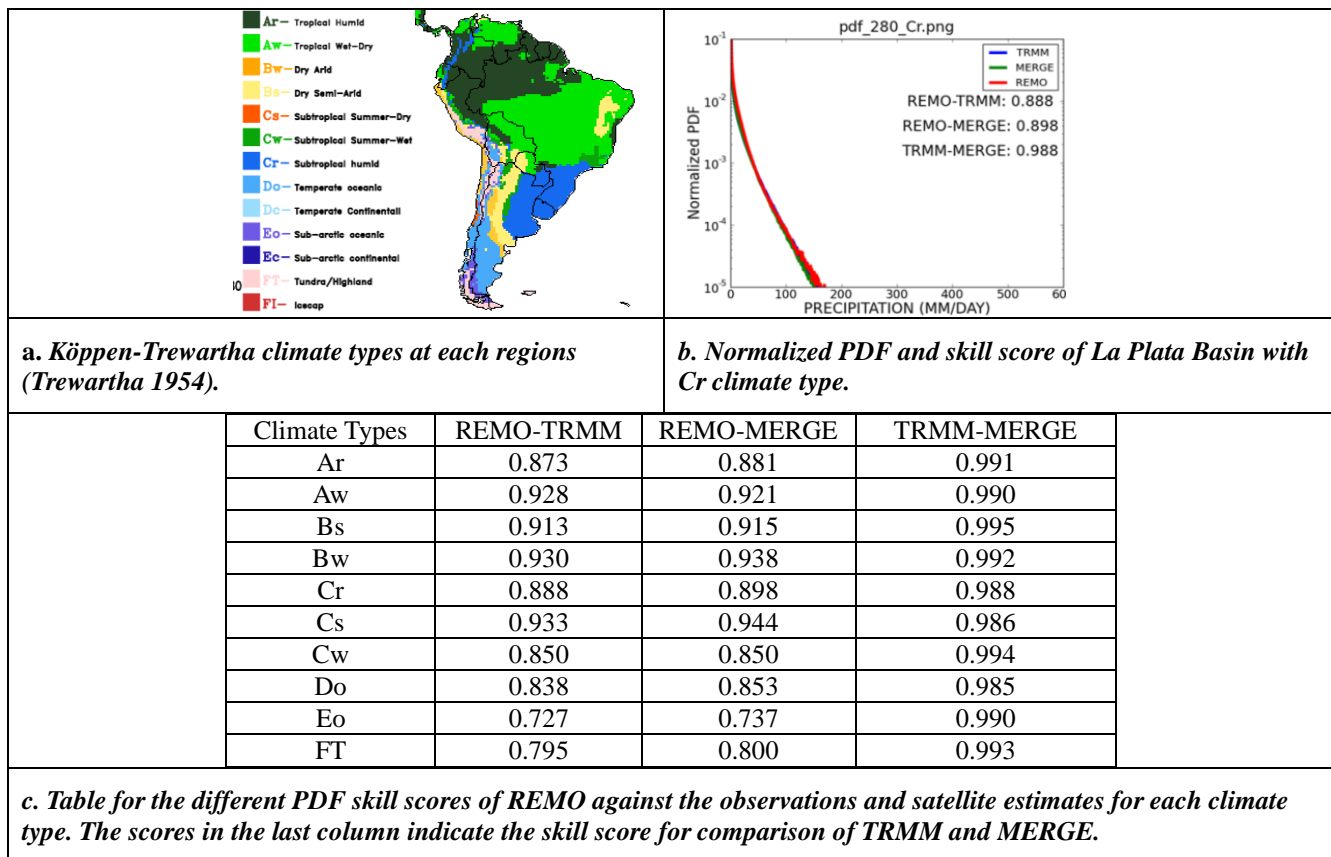


Figure 10. Method for calculating the skill of the model using empirical distribution functions.

**Mesoscale convective systems.** The characteristics of the mesoscale convective systems are analyzed using the outgoing long-wave radiation and daily precipitation. In tropical and subtropical regions of the continent, low values of outgoing longwave radiation indicate deep convection. Satellite estimates of the outgoing longwave radiation from NCEP-NCAR at a horizontal resolution of  $2.5^\circ \times 2.5^\circ$  (Liebmann and Smith, 1996) are used to compare with our model results. The spatial characteristics of the model results are similar to the OLR estimates but the magnitude in the model is higher compared to the observations (figure not shown).

The daily precipitation distribution of the model is evaluated during the last decade of the simulation period from 1999 to 2008. The simulated daily precipitation on regions with similar climate types are compared against satellite estimates from TRMM 3B42 (Huffman et al, 2007) and MERGE (Rozante, et al, 2010). TRMM has a resolution of  $0.25^{\circ} \times 0.25^{\circ}$ . MERGE is a hybrid data based on TRMM estimates merged with the rain gauge observations over South America at a resolution of  $0.2^{\circ} \times 0.2^{\circ}$ . The skill of the model is calculated using empirical probability distribution functions (Perkins et al, 2007) as shown in Figure 10. The figure shows that the model has a reasonable skill in simulating the daily precipitation distribution within regions of similar Köppen-Trewartha climate types (Trewartha, 1954). In the La Plata Basin (Cr-climate type), REMO has a high skill score compared with TRMM and MERGE.

Mesoscale convective systems are also characterized by heavy precipitation events. In this study, we have considered the 95<sup>th</sup> percentile of the whole daily rainfall distribution during summer (DJF) as a threshold of heavy precipitation events. The intensity and frequency of heavy precipitation in the model and observations are shown in Figure 11. The intensity simulated by the model is similar to the observations while the frequency of heavy precipitation are slightly higher in the model compared to TRMM and MERGE.

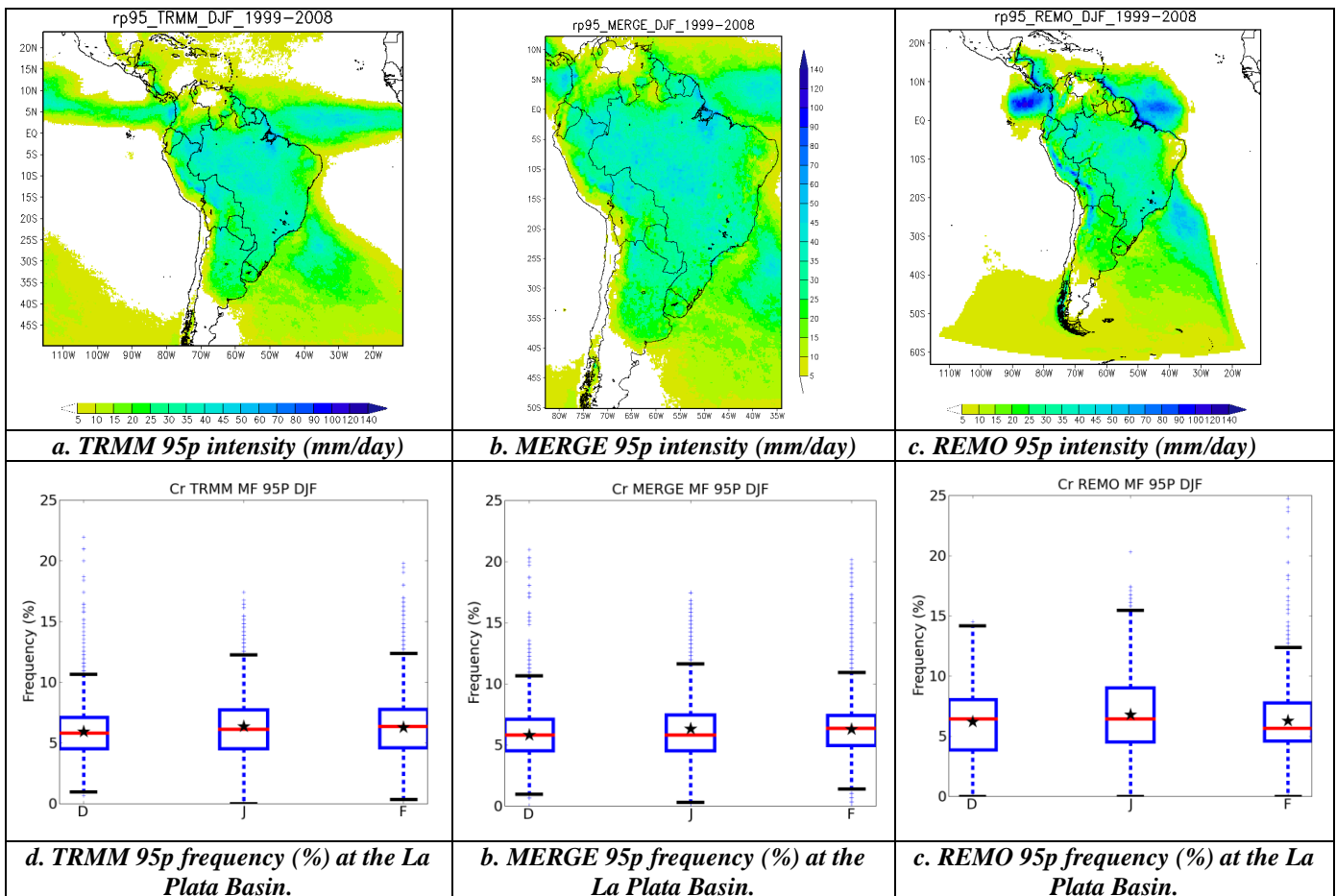


Figure 11. Heavy precipitation threshold (95th percentile) intensity (a-c) and frequency (d-f) during summer (DJF) 1999-2008. – In collaboration with INPE/CPTEC (Iracema Cavalcanti)

REFERENCES:

- da Silva, M.; da Rocha, R. & Ynoue, R. Climatic simulations of the eastern Andes low-level jet and its dependency on convective parameterizations *Meteorology and Atmospheric Physics*, Springer Wien, 2010-09-01, 108, 9-27.
- Huffman, G.J., R.F. Adler, D.T. Bolvin, G. Gu, E.J. Nelkin, K.P. Bowman, Y. Hong, E.F. Stocker, D.B. Wolff, 2007: The TRMM Multi-satellite Precipitation Analysis: Quasi-Global, Multi-Year, Combined-Sensor Precipitation Estimates at Fine Scale. *J. Hydrometeorol.*, 8(1), 38-55.
- Jacob, D.; 2001: A note to the simulation of the annual and inter-annual variability of the water budget over the Baltic Sea drainage basin. *Meteorology and Atmospheric Physics*, Vol.77, Issue 1-4, 61-73.
- Liebmann B. and C.A. Smith, 1996: Description of a Complete (Interpolated) Outgoing Longwave Radiation Dataset. *Bulletin of the American Meteorological Society*, 77, 1275-1277.
- Marengo, J. A.; Soares, W. R.; Saulo, C. & Nicolini, M. Climatology of the Low-Level Jet East of the Andes as Derived from the NCEP-NCAR Reanalyses: Characteristics and Temporal Variability *J. Climate, Journal of Climate*, American Meteorological Society, 2004, 17, 2261-2280.
- Perkins, S.E., A.J. Pitman, N.J. Holbrook and J. McAneney, 2007, Evaluation of the AR4 Climate Model's Simulated Daily Maximum Temperature, Minimum Temperature, and Precipitation over Australia using Probability Density Functions, *J. Climate*, 20, 4356- 4376.
- Rozante, J. R., and I. F. A. Cavalcanti (2008), Regional Eta model experiments: SALLJEX and MCS development, *J. Geophys. Res.*, 113, D17106, doi:10.1029/2007JD009566.
- Rozante, J. R.; Moreira, D. S.; de Goncalves, L. G. G. & Vila, D. A. Combining TRMM and Surface Observations of Precipitation: Technique and Validation over South America, *Wea. Forecasting, Weather and Forecasting*, American Meteorological Society, 2010, 25, 885-894
- Salio, P.; Nicolini, M. & Zipser, E. J. Mesoscale Convective Systems over Southeastern South America and Their Relationship with the South American Low-Level Jet, *Mon. Wea. Rev., Monthly Weather Review*, American Meteorological Society, 2007, 135, 1290-1309
- Vera, C.; Baez, J.; Douglas, M.; Emmanuel, C. B.; Marengo, J.; Meitin, J.; Nicolini, M.; Nogue-Paegle, J.; Paegle, J.; Penalba, O.; Salio, P.; Saulo, C.; Silva Dias, M. A.; Silva Dias, P. & Zipser, E. The South American Low-Level Jet Experiment. *Bulletin of the American Meteorological Society*, 2006, 87, 63 – 77
- Trewarth, G.T.; *An Introduction to Climate*, 3<sup>rd</sup> ed., New York, McGraw-Hill, 1954.